URN

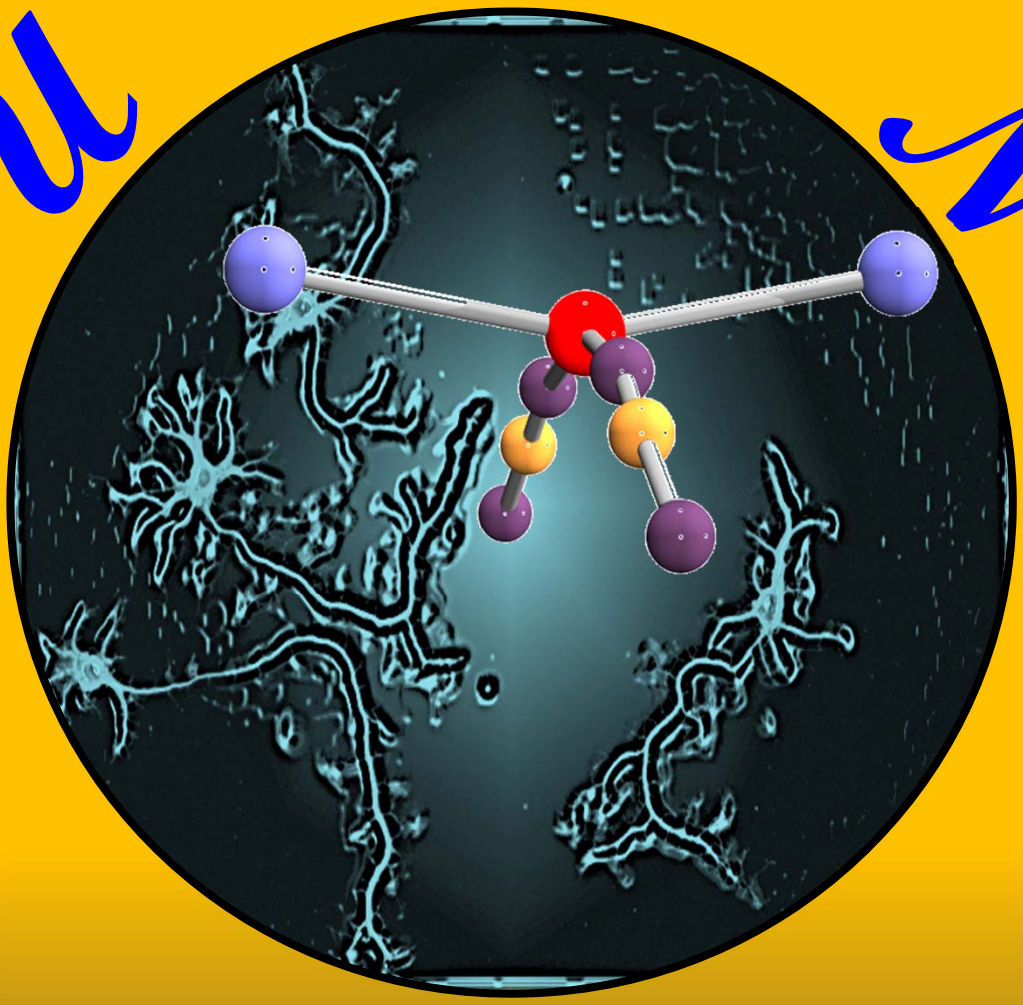

UNIVERSITY OF MIAMI

Undergraduate Research Newsletter

May 2011

Volume 2

Issue 1

EDITORS

REVIEW BOARD

Special Thanks

Office of Undergraduate Research and Community Outreach

Available Online: For more information please visit the URN homepage under the Office of Undergraduate Research webpage at www.miami.edu

Table of Contents

Foreword

It is my great pleasure to write the introduction to this second issue of the Undergraduate Research Newsletter (URN), which showcases research from undergraduates here at the University of Miami (UM). Undergraduate research provides an important bridge between the classroom experience, where the student solves problems with known solutions, and the laboratory experience, where problems with unknown solutions are tackled with no guarantee of success. For me personally, undergraduate research greatly influenced my decision to pursue a career in science and tempered my expectations of scientific research. My first experience with undergraduate research was during the summer after my freshman year at Caltech in the lab of Dr. John D. Roberts, a pioneer in the application of NMR to organic chemistry. My project was to determine the effect of solvent on the molecular conformation of β-alanine by analyzing changes in scalar coupling measured using nuclear magnetic resonance (NMR). I was excited to apply my knowledge of NMR, which I had recently learned about in my organic chemistry course, to an actual research problem. As with most research, things did not go as smoothly as planned. Although unable to make much headway in my main project, I synthesized a β-alanine derivative on a side project that was subsequently used by others in a related NMR study. This resulted in an authorship on my first paper many years later. While unsuccessful in solving the main research question, I did find that I enjoyed NMR and its theoretical framework. I eventually ended up pursuing my Ph.D. in NMR at Berkeley, and my current research program focuses on developing new NMR techniques.

In this URN, the reader will get a glimpse of the research UM undergraduates are working on in a variety of disciplines in the natural and social sciences. The work represents original research that has undergone a review process by UM Faculty in a manner similar to that found in scholarly journals. The breadth of research is quite extraordinary, ranging from a study on the effects of energy and expectations on distance perception to an analysis of the experimentally measured cosmic microwave background. I hope that the authors will find their undergraduate research experience, the fruit of which is distilled here in these pages, a useful guide in their life.

Jamie Walls
Assistant Professor, Chemistry

Blood Monocytes From Mammary Tumor-Bearing Mice: Early Targets of Tumor-Induced Immune Suppression?

Raul Caso (Class of 2011)

Major: Microbiology and Immunology
Principal Investigator/Supervisor: Dr. Marta Torroella-Kouri
Department: Microbiology and Immunology
Senior Thesis: Yes

Peritoneal macrophages from mice bearing advanced mammary tumors are impaired in their inflammatory functions. However, little is known about whether similar defects exist in their precursor stages as blood monocytes. Mononuclear cells were isolated from whole blood of D1-DMBA-3 mammary tumor-bearing and normal BALB/c mice and CD115$^+$ monocytes were analyzed. Our results show that there is an increase in circulating monocytes in tumor hosts; exhibiting a reduced expression of several key myeloid differentiation markers such as CD115, F4/80, CD68 and CD11b. Furthermore, gene microarray analysis performed for the first time in blood monocytes from tumor hosts indicates that they express a mixture of pro-inflammatory and anti-inflammatory cytokines and chemokines. Importantly, complement proteins are enhanced whereas nitric oxide production is decreased and there is no measurable arginase activity detected in these cells. Collectively, this study represents the first comprehensive analysis of blood monocytes from tumor-bearing mice; it concludes that these cells are neither completely inflammatory nor suppressive and are less differentiated, similar to the macrophages they later become.

Inflammation and immune suppression are two opposing immune responses linked in different ways to cancer: while earlier stages of tumor development are associated with chronic inflammation[1], later stages of tumor progression are characterized by tumor-induced immune suppression[2]. Macrophages are key players of the inflammatory response and exhibit significant roles in the different stages of tumor development; their release of mutation-inducing free radicals as part of their inflammatory response contributes to tumor initiation, while their secretion of factors that promote angiogenesis, invasion, extracellular matrix remodeling and metastasis plays important roles in tumor progression. However, while tumor development is modulated by macrophages, the function of macrophages is likewise altered by the tumor resulting in macrophages that exhibit immune suppressive traits thereby contributing to tumor progression[3].

Circulating blood monocytes are the precursors of tissue macrophages. Monocytes are released into the peripheral blood where they circulate before entering tissues and replenishing tissue macrophage populations[4]. They constitute a group of immune effector cells, equipped with chemokine and adhesion receptors which mediate their migration from blood to tissues during infection or homeostasis[5]. Monocytes show the ability to recognize lipids and various microorganisms, and once stimulated they can produce large quantities of factors involved in the elimination of foreign objects as a consequence of their inflammatory response. Although extensive data has been collected describing the functions of monocytes during inflammation due to infection, evidence is lacking regarding the characteristics of monocytes in the context of tumor burden. We have previously shown that peritoneal macrophages from mice bearing advanced mammary tumors are defective in their inflammatory response[6]. In the present work we addressed the challenge of characterizing a cell population present in low percentages in the blood, as monocytes are, and performed a broad analysis of these cells in tumor-bearing mice as compared to their normal counterparts.

We investigated whether CD115$^+$ blood monocytes from tumor-bearing mice are defective prior to differentiating into macrophages within tissues. Mononuclear cells were isolated from the whole blood of D1-DMBA-3 mammary tumor-bearing and normal BALB/c mice. Monocytes were then isolated using their expression of the CD115 receptor on their outer membrane. Our data has corroborated that tumor hosts exhibit an alteration in

myelopoiesis, leading to an accumulation of monocytes in the blood, as has been described by us and others[6,7]. Our analysis of the blood monocyte population in tumor-bearing mice shows a substantial increase in the *percentage* of circulating CD115$^+$ monocytes (Figure 1A). This increase may be a result of enhanced myelopoiesis within the bone marrow of tumor hosts and has been associated with the action of factors released by the tumor itself as well as an increase in the death of tissue macrophages[6].

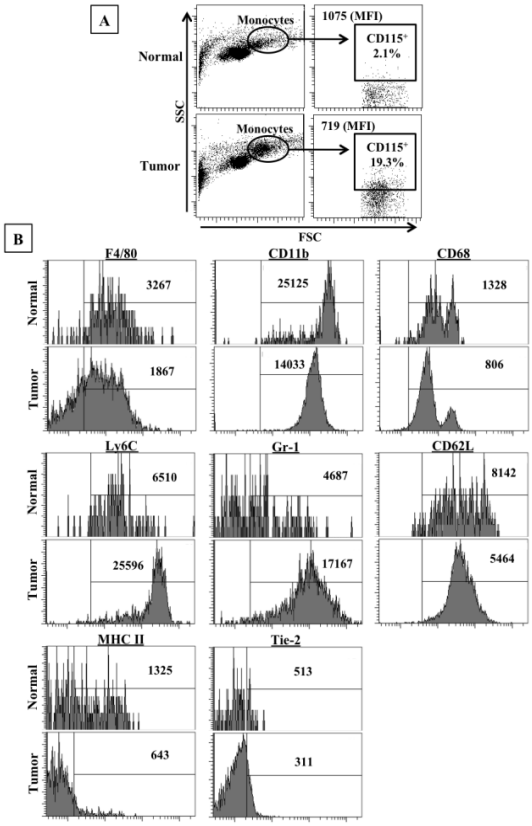

Figure 1: Monocytes from tumor-bearing mice are more numerous and less differentiated. **A**, Analysis of CD115 expression by monocyte population obtained from the mononuclear cell fraction of peripheral blood from tumor-bearing mice, *bottom right*, and normal mice, *top right*. **B**, Analysis of the expression of F4/80, CD11b, CD68, Ly6C, Gr-1, CD62L, MHC II, and Tie-2 by CD115$^+$ blood monocytes obtained from normal, *top*, and tumor-bearing mice, *bottom*.

In addition, CD115$^+$ blood monocytes from tumor-bearing mice down-regulate their expression of CD115, CD11b, F4/80, and CD68 (Figure 1B), indicating that they exhibit a more immature phenotype compared to their healthy counterparts. Interestingly, our analysis of the mRNA transcripts expressed by these cells revealed that CD115$^+$ blood monocytes from tumor hosts express a mixture of pro- and anti-inflammatory traits (Table 1).

Gene Name	Gene Symbol	Constitutive Expression (fold change)	LPS-induced Expression (fold change)
Pro-inflammatory response			
Interleukin 12 alpha	*Il12a*	61.99	137.39
Complement component 3	*C3*	39.51	78.56
Tumor necrosis factor	*Tnf*	19.57	4.05
Interleukin 18	*Il18*	16.83	19.29
Chemokine (C-C motif) receptor 2	*Ccr2*	15.27	7.78
Toll-like receptor 4	*Tlr4*	15.09	9.12
Chemokine (C-C motif) ligand 2	*Ccl2*	13.57	68.71
RAS-related C3 botulinum substrate 1	*Rac1*	7.64	25.38
Myeloid differentiation primary response gene 88	*Myd88*	6.89	3.23
Nuclear factor kappa light chain	*Nfkb*	6.72	-
Nitric oxide synthase 2, inducible, macrophage	*Nos2*	5.37	11.28
Interferon alpha	*Ifna*	-	-57.03
Interleukin 1 beta	*Il1b*	-2	-2.13
Interleukin 6 signal transducer	*Il6st*	2.38	-11.18
Anti-inflammatory response			
Interleukin 10	*Il10*	-	35.71
Interleukin 10 receptor, beta	*Il10rb*	9.83	3.87
Interleukin 1 receptor antagonist	*Il1rn*	17.64	44.33
Interleukin 1 receptor, type II	*Il1r2*	-	2.28
Interleukin 13 receptor, alpha 1	*Il13ra1*	45.22	68.43
Interleukin 1 alpha	*Il1a*	16.92	74.48
Chemokine (C-C motif) ligand 24	*Ccl24*	17.14	9.68
Other genes of interest			
Cytoplasmic FMR1 interacting protein 2	*Cyfip2*	47.38	134.08
Hypoxia inducible factor 1, alpha subunit	*Hif1a*	18.34	4.31
Chemokine (C-X3-C motif) receptor 1	*Cx3cr1*	8.98	-
Chemokine (C-X3-C motif) ligand 1	*Cx3cl1*	3.29	2.21

Table 1: Transcripts expressed in CD115$^+$ blood monocytes obtained from tumor-bearing mice.

We also provide evidence that CD115$^+$ blood monocytes from tumor-bearing mice over-express complement, such as C3 and C5a receptor (Figure 2), which play critical roles in the immune response and can be exploited by the tumor in order to create an immunosuppressive environment[8], thus resulting in persistent tumor growth. Moreover, monocytes from tumor-bearing mice are defective in their production of nitric oxide (Figure 3A), which is produced in response to the presence of microorganisms and foreign objects. Also, the lack of measurable arginase activity (Figure 3B) in these cells, together with their phenotype, indicates that, by definition, they are not phenotypically part of a group of undifferentiated heterogeneous myeloid cells that have been described in tumor-bearing mice, the myeloid-derived suppressor cells (MDSCs)[9].

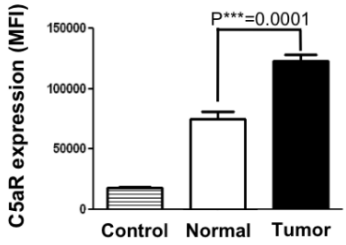

Figure 2: C5a receptor is upregulated in monocytes from tumor bearers. Analysis of the expression of C5a receptor (C5aR) by $CD115^{+}$ blood monocytes from normal and tumor-bearing mice.

All together, we conclude that blood monocytes from mammary tumor-bearers are neither completely pro-inflammatory nor anti-inflammatory. Rather, they exhibit characteristics of both activation profiles.

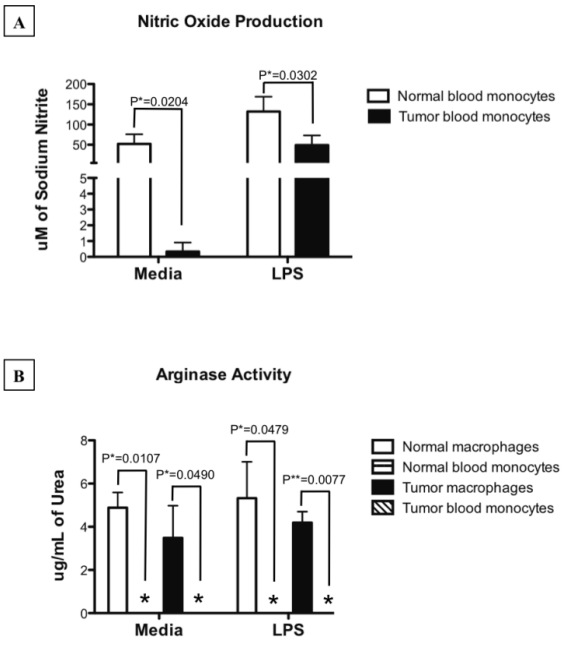

Figure 3: Blood monocytes from tumor-bearers exhibit a defective production of nitric oxide (NO) compared to normal mice and no measurable arginase activity. **A**, Analysis of the nitric oxide production by $CD115^{+}$ blood monocytes from normal and tumor-bearing mice. **B**, Determination of the amount of urea detected in µg/mL as an indication of arginase activity within $CD115^{+}$ blood monocytes from normal and tumor-bearing mice.

Much effort is currently devoted to reversing macrophages' adverse traits in tumor hosts; being cells that reside within tissues, access, for therapeutic purposes, is limited. Thus, defective blood monocytes could be better targeted and manipulated by less invasive means because of their location in the peripheral circulation of the tumor host. Importantly, the exposure of monocytes and peritoneal macrophages to circulating tumor factors may be responsible for cell alterations in tumor hosts. Perhaps increased production of tumor factors may affect the normal pathway of cell differentiation resulting in the accumulation of immature monocytes in the blood of tumor-bearing mice[10]. Consequently, blocking these tumor factors may prove effective in reverting tumor-induced immune suppression in monocytes and macrophages residing within tumor-bearing hosts.

References

[1] F. Balkwill, K.A. Charles, and A. Mantovani (2005). "Smoldering and polarized inflammation in the initiation and promotion of malignant disease" Cancer Cell 7, 211-217.
[2] A. Mantovani, S. Sozzani, M. Locati, P. Allavena, and A. Sica (2002). "Macrophage polarization: tumor-associated macrophages as a paradigm for polarized M2 mononuclear phagocytes" Trends Immunol 23, 549-555.
[3] B.Z. Qian and J.W. Pollard (2010). "Macrophage diversity enhances tumor progression and metastasis" Cell 141, 39-51.
[4] S. Gordon and P.R. Taylor (2005). "Monocyte and macrophage heterogeneity" Nat Rev Immunol 5, 953-964.
[5] F. Geissmann, M.G. Manz, S. Jung, M.H. Sieweke, M. Merad, and K. Ley (2010). "Development of monocytes, macrophages, and dendritic cells" Science 327, 656-661.
[6] M. Torroella-Kouri, R. Silvera, D. Rodriguez, A. Shatry, R. Caso, S. Opiela, N. Strbo, Y. Cardentey, R.A. Schwendener, V. Iragavarapu-Charyulu, and D.M. Lopez (2009). "Identification of a Subpopulation of Macrophages in Mammary Tumor-Bearing Mice That Are Neither M1 nor M2 and Are Less Differentiated" Cancer Res 69, 4800-4809.
[7] G. Gallina, L. Dolcetti, P. Serafini, *et al* (2006). "Tumors induce a subset of inflammatory monocytes with immunosuppressive activity on CD8+ T cells" J Clin Invest 116, 2777-2790.
[8] M.M. Markiewski, R.A. DeAngelis, F. Benencia, *et al* (2008). "Modulation of the antitumor immune response by complement" Nat Immunol 9, 1225-1235.
[9] S. Ostrand-Rosenberg and P. Sinha (2009). "Myeloid-derived suppressor cells: linking inflammation and cancer" J Immunol 182, 4499-4506.
[10] B. Almand, J.I. Clark, E. Nikitina, *et al* (2001). "Increased production of immature myeloid cells in cancer patients: a mechanism of immunosuppression in cancer" J Immunol 166, 678-689.

Calorimetric Study on the Heat of Binding of Chlorine to a Dual Platinum Core Compound

Megan Chui (Class of 2012)

Major: Chemistry
Principal Investigator/Supervisor: Dr. Carl Hoff
Department: Chemistry
Fellowship/Awards/Recognition: College of Arts and Sciences Summer Research Program for Underrepresented Minorities and Women
Senior Thesis: Yes

Reactions involving Chlorine gas have not been extensively studied due to its toxic nature. A custom, airtight calorimetry system was built to measure the heat of binding of chlorine to a dual platinum core compound. The calorimeter was successfully calibrated to measure the change in temperature in order to calculate the enthalpy of formation using Hess's Law. The study found the solubility of the platinum compound in carbon tetrachloride (CCl_4) to be very poor thus not fully reacting. In future experiments, Chlorine will as at the limiting reagent and will be added to a Platinum solution. This modification in the procedure will hopefully provide more accurate results.

The purpose of these experiments was to determine the heat of binding of chlorine (Cl_2) to a dual platinum core compound through calorimetric studies. The research is done in conjunction with Dr. Tim Cook and Dr. Daniel Nocera from Massachusetts Institute of Technology. The study of chlorine-metal bonding is integral in the production and storage of solar energy and will provide information for other Chlorine-metal catalysis.

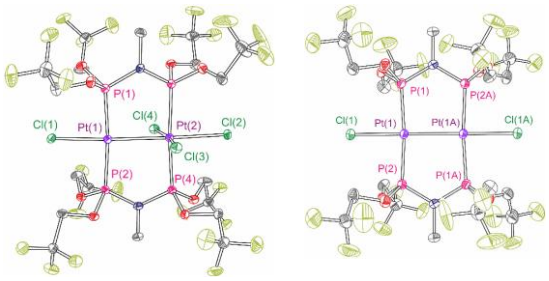

Figure 1: $Pt_{(1,1)}$ and $Pt_{(1,2)}$ structure

The measured heats of reaction are summarized in Table 1.

	ΔH_{RXN} (kcal/mol)	
$Pt_{(I)} - Pt_{(I)} + 2Cl_2 \rightarrow Pt_{(III)} - Pt_{(III)}$	-60	(A)
$Pt_{(I)} - Pt_{(III)} + Cl_2 \rightarrow Pt_{(III)} - Pt_{(III)}$	-35	(B)
$Pt_{(I)} - Pt_{(III)} + Pt_{(III)} - Pt_{(III)} \rightarrow 2Pt_{(I)} - Pt_{(III)}$	-10	(C)

Table 1. Approximate heats of reaction based on limited data.

The enthalpies of chlorination were measured using an airtight glove box in which the calorimeter was completely contained. The calorimeter was built by Allison Ring and described in a previous issue of URN[1]. As discussed later, all of the data in Table 1 is subject to experimental error and additional study will have to be done on these reactions. The first job was to calibrate the calorimeter system to make sure that this newly constructed calorimeter gave reliable and reproducible data. This was done by using precision electrical heat input and testing the response of the system to variables such as rate of stirring and solvent. This was successful and a chemical calibration was done utilizing the reaction shown in Table 2.

$$PCl_3 + Cl_2 \rightarrow PCl_5$$

Trial	Weight of PCl_3 (g)	ΔH_{RXN}(kcal/mol)
1	0.1045	-18.42
2	0.1973	-19.41
3	0.0944	-17.67

Table 2. Measured heat of reaction of Cl_2 and PCl_3, Results.

There was considerable difficulty and even risk in making these measurements. Laboratory grade chlorine gas is extremely toxic and corrosive garnering a position in Toxicity Category I, the highest degree of acute toxicity by the Environmental Protection Agency[2]. The inhalation of Cl_2 results in bronchitis, asthma, heart disease, meningitis, and is sometimes fatal. The reaction is contained in an airtight glove box, however gas masks with chlorine cartridges

were worn throughout the experiment, see Figure 2.

Figure 2. The author (left) graduate student Xiaochen Cai(center) and Subhojit Majumdar(left) wearing gas masks during calorimetry experiments.

A major reason the results in Table 1 need to be repeated is uncertainty in the amount of material reacting in the measurements. Custom ampoules were created and filled with the platinum complex and sealed under Argon gas. Small glass rods wrapped with Teflon tape were pushed down the neck to reduce the amount of residue on the sides of the ampoule and plug the ampoule. In spite of that, examination of the broken ampoules at the end of the experiment revealed that not all of the sample went into solution. A red colored residue was often seen on the stem and upper parts of the ampoule. This is due primarily to the poor solvation properties of CCl_4. Due to the fact that Cl_2 attacks most solvents other than CCl_4 (which is already fully chlorinated) this was the only solvent suitable for these studies. However, the dinucler Pt complexes did not dissolve well in CCl_4 and while the data in Table 1 provide a "first look" at the reaction energies, this work is scheduled to be repeated summer 2011.

In repeating the work the procedure will be reversed. Instead of adding Pt to a solution of Cl_2, ampoules of Cl_2 will be added to a previously prepared solution of the Pt complex. This should result in rapid reaction and more accurate calorimetry. In addition it will avoid the possibility of over oxidation by excess Cl_2 since Cl_2 will now be the limiting reagent.

The fact that the data need repeating is made clear by the measured value of reaction (c) in Table I. Using Hess's law, A-2B = C for the reaction, and also for the enthalpy. Using these data, we calculate -60 - 2(-35) = +10 kcal/mol, not -10 kcal/mole. In doing difficult measurements it is always important to make a check. Reaction C, which we discovered during this project, provides an excellent check on the data. In this case telling us that the work, though possibly close to be correct is not yet publishable.

A final note of interest is the much more exothermic reaction of $Pt(PR_3)_2$ (R = tertiary butyl or cyclohexyl). These complexes were more soluble in CCl_4 and did not present the difficulties of the dinuclear Pt complexes. These complexes reacted with Cl_2 and were exothermic by more than 100 kcal/mol. The products of oxidation of Pt by Cl_2 in Table 1 are $Pt_{(III)}$, so the energies measured correspond to $Pt_{(I)} + Cl_2 \rightarrow Pt_{(III)}Cl_2$, as opposed to $Pt_{(0)} \rightarrow Pt_{(II)}$ for the PR_3 complexes.

One problem in these measurements is that either the cis or the trans structure of the platinum molecule could be formed. NMR spectral data will allow us to distinguish between the two structures shown in Figure 3. It is of interest to determine these differences in energy as well. If the complex shown in Figure 3 and NR_3 rather than PR_3 ligands it would be "cisplatin" which is one of the most widely used anti-cancer drugs[3].

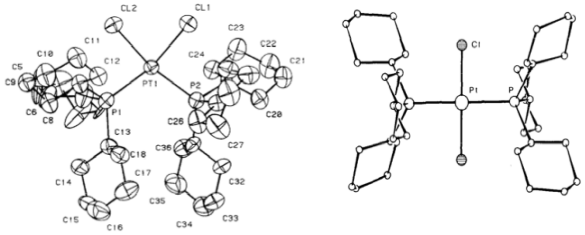

Figure 3: The molecular structure of cis (left) and trans - $Cl_2Pt(PCy_3)_2Cl_2$[4].

In spite of apparent failure in getting accurate data, a world of experience was gained in dealing with small quantities of expensive Pt complexes as well as handling, manipulating, and safely disposing of Cl_2. The fact that there is such a big difference in enthalpies of binding makes this a project worth doing--even though at this time exactly how much more exothermic the $Pt_{(0)} \rightarrow Pt_{(II)}$ reactions are than the $Pt_{(I)} \rightarrow Pt_{(III)}$ reactions. The discovery of reaction c in Table 1 provides a good means to check the reaction. Finally, the glove box system developed by Allison Ring was proved to work[1].

References

[1] A. Ring (2010) "Chlorine Calorimetry within an Air Tight Environment" University of Miami Undergraduate Research Newsletter, 1, 16-18.
[2] Environmental Protection Agency. "R.E.D. Facts: Chlorine Gas" http://www.epa.gov/oppsrrd1/REDs/factsheets/4022fact.pdf Aug. 2010
[3] T. A. Cameron, H.C. Clark, A. Linden, and A.M. Nicholas (1989) " Inorganica Chimica Acta, 162, 9-10.
[4] A. Del Pra, and G. Zanotti (1980) Inorganica Chimica Acta, 39, 137-141.

Situational Influences on Children's Compliance Behavior: The Effects of Temperament and Parenting

Irene Daboin (Class of 2011)

Major: Psychology
Principal Investigator/Supervisor: Dr. Heather Henderson
Department: Psychology
Senior Thesis: Yes

The current study examines the influence of within-child factors (temperamental effortful control) and socialization factors (parenting behavior) on children's compliance, both independently and in combination. Data was collected from 247 children, age five, and detailed coding of children's observed behaviors during an individual compliance task (Prohibited Toy) and a social compliance task (Clean-Up), as well as maternal self-report of child-rearing practices, and maternal report of children's temperament. We ran a multiple regression analysis and found a goodness-of-fit interaction in the individual task, such that children whose parents responded appropriately to children's low effortful control with either high nurturance or high restrictiveness displayed the best developmental outcomes. In the social task, there was a main effect of temperamental effortful control, but no effects of parenting, which leads us to suspect that within-child factors have a greater influence than socialization factors on children's behaviors during social interactions with peers.

Compliance is defined as a child's ability to respond appropriately to an adult request.[1] Previous research shows that compliance relates to socio-emotional competence later in life and is influenced by both within-child factors (i.e., temperament) and socialization (i.e., parenting).[2]

Temperament has been defined as the emotional, motor and attentional differences in a child's reactivity and self-regulation.[3] Reactivity refers to the individual's responses and arousability to stimuli; how strong, fast, positive, or negative these are. Self-regulation refers to the individual's control over his/her behaviors and emotions in reaction to stimuli.[4] Effortful control is a type of self-regulation that is positively associated with compliance, and is defined as the voluntary capacity to restrain a dominant response in order to enact a more appropriate subdominant response.[5]

Parenting has also been associated with children's compliance behaviors. Specifically, parental nurturance and support have been found to be related to children's compliance, and restrictiveness and power assertion have been associated with children's non-compliance.[6] Studies have also shown that consistent parenting and appropriate reactions produce a family environment that leads to child compliance, no matter the parenting style.[7] This leads us to believe that both restrictive and nurturing parenting could possibly yield high levels of compliance and low levels of defiance.

The current study sought to examine the moderating effects of parenting on the relation

between temperament and compliance in 5-year-old-children. We predicted that high temperamental effortful control, high nurturing parental behavior, and high restrictive parenting would be independently associated with greater compliance and less defiance across contexts. We also expected there would be an interaction between temperamental effortful control and parenting, such that that high nurturing and high restrictive parenting behaviors, when paired with low effortful control, would yield more compliance and less defiance. In addition, since few studies have examined these effects across contexts, this study included both social and non-social compliance tasks to examine whether context influences the associations between the constructs.

Data was collected from 247 participants at the age of five, during two different laboratory sessions. During the first session, children were asked to complete an individual compliance task in which they were told by the experimenter to sort beads into bins by color, while abstaining from playing with any of the age-appropriate and attractive toys in the room. During this visit, participants' mothers were asked to complete a self-report questionnaire about their child rearing practices. During the second session, participants were paired with a same sex, unfamiliar peer to complete a social compliance task in which both children were asked to put away a set of age-appropriate and attractive toys, after having had approximately ten minutes of free play. During this visit, participants' mothers were asked to complete a questionnaire about their child's temperamental effortful control.

We ran a multiple regression analysis and found that in the individual compliance task there were no main effects of effortful control or parenting on child compliance. However, when examining defiance during this task, there was an interaction between effortful control and parenting. Specifically, given the presence of high maternal restrictiveness or nurturance, low temperamental effortful control was associated with high defiance, and high temperamental effortful control was associated with low defiance. This finding suggests that the best developmental outcomes are a result of the goodness-of-fit between specific parenting styles and children's unique levels of self-regulation.

In the social compliance task, we found that there was a main effect for effortful control both on compliance and defiance, such that children high on effortful control displayed more compliance and less defiance. However, we found no main effects for parenting or interactions. This leads us to believe that in the social setting, within child factors have a greater influence on developmental outcomes than do socialization factors.

For future directions, we suggest that studies examine how other within-child factors interact with parenting and how peer comments and behaviors during a compliance task may influence child behaviors. For example, it may be that temperamental self-regulation affects behavior during social tasks in part through the effects it has on susceptibility to peer influences (either positive or negative). Furthermore, because our study only examined children at age five, we suggest examining multiple ages to better understand the development of compliance over time.

References

[1] G. Kochanska (1993). "Toward a synthesis of parental socialization and child temperament in early development of conscience" Child Development, 64(2), 325-347.

[2] G. Kochanska (1991). "Socialization and temperament in the development of guilt and conscience" Child Development, 62(6), 1379-1392.

[3] D. Derryberry, and M. K. Rothbart (1997). "Reactive and effortful processes in the organization of temperament" Development and Psychopathology, 9(4), 633-652.

[4] H. A. Henderson, and T. D. Wachs (2007). "Temperament theory and the study of cognition-emotion interactions across development" Developmental Review, 27(3), 396-427.

[5] G. Kochanska, and A. Knaack (2003). "Effortful control as a personality characteristic of young children: Antecedents, correlates, and consequences" Journal of Personality, 71(6), 1087-1112.

[6] S. Crockenberg, and C. Litman (1990). "Autonomy as competence in 2-year-olds: Maternal correlates of child defiance, compliance, and self-assertion." Developmental Psychology, 26(6), 961-971.

[7] R. G. Wahler, and K. L. Meginnis (1997). "Strengthening child compliance through positive parenting practices: What works?" Journal of Clinical Child Psychology, 26(4), 433-440.

Identification of Positively Selected Sites In HIV1 Vif

Harold Gil (Class of 2011)

Majors: Chemistry, Biochemistry and Molecular Biology
Principal Investigator/Supervisor: Dr. Rik Myers
Department: Biochemistry and Molecular Biology
Fellowship: Cuban Heritage Collection
Senior Thesis: No

The HIV1 Vif protein suppresses the viral inhibitory effects of endogenous restriction factors such as APOBEC3G. A Bayesian statistical analysis of twenty Vif DNA sequences is yielding insights into the evolution and positive selection of specific amino acid residues. Fourteen positively selected residues have been identified in Vif and mapped onto its crystal structure. These sites will be compared with biochemical and structural data from the literature to determine if these sites correspond to those suggested to be involved in the Vif-APOBEC3G interaction. This study will improve our understanding of Vif evolution and identify specific residues that can be targeted for therapeutic drug solutions to HIV.

HIV's viral infectivity factor (Vif) has received considerable attention since the discovery that HIV particles lacking, or containing defective, Vif largely fail to establish infection in nonpermissive cells (T-lymphocytes, macrophages, CEM, among others)[1]. The innate antiviral defense of nonpermissive cells was attributed to the APOBEC3G restriction factor proteins. APOBEC3G has roles in the hypermutation of the viral cDNA, destabilization of the pre-integration complex, and inhibition of viral transposition.[2] Vif suppresses intracellular levels of APOBEC3G by proteasomal degradation through an E3 ubiquitin ligase complex, thus promoting HIV infection.[3] The Vif-APOBEC3G axis could, therefore, serve as a potential therapeutic drug target by limiting Vif-induced degradation of APOBEC3G, resulting in decreased viral infection.[3]

This goal of this research is to identify the amino acid residues of Vif that are under positive selection and then map them onto Vif's 3-D crystal structure to identify loci of high variability. Positive selection is a process in which the rate of nonsynonymous substitution is greater than that of synonymous substitution;[4] it implies that these residues are under selective pressure to change, perhaps to evade endogenous restriction factors.

The identification of positively selected sites was carried out using the Bayesian statistical software, MrBayes. Twenty Vif DNA sequences were taken from the HIV Sequence Database. The DNA sequence data was analyzed by employing a General Time Reversible/Codon model. This model sets a proportion of codon sites to be invariable and provides for a gamma-shaped distribution of substitution rates across sites. Two independent computational calculations were run under this model and convergence of the calculations was diagnosed when the average standard deviation in partition frequency values between the two independent calculations reached a value of, or below, 0.01. Among the properties of the system that were calculated were the probabilities of positive selection of individual residues. The results of the converged calculations yielded 43 sites in Vif with a probability >90% of having been positively selected.

Res	PS	G	A	V	L	M	I	S	T	C	P	N	Q	F	Y	W	K	R	H	D	E
37	.99	X										2					4			1	2
39	.99			4	2			1		1				X							
47	.99				1		1	1			X							15			
65	.99					1	1					X					4				1
76	1		2				1		X		4										
94	1	1										1					X	2			2
124	.99											2					X	2			1
129	.99											1	9					3	X		2
134	.99						2	6				X					2				
138	.99							2			3		X					1	1		
158	.99		3						X								1				1
160	.99						1		9								X				1
167	.99						X		9		1							3			4
175	.99								X				1				2	15			1

Figure 1: Res=Residue #, PS= Probability of positive selection, X=wild-type residue.

These sites were then analyzed- those with the highest degree of variability in the chemical properties (nonpolar, polar, aromatic, basic, or acidic) of the corresponding residues for the sites were taken to be the most likely sites for undergoing positive selection. The 14 residues most likely to be undergoing positive selection are listed below in Figure 1 along with their probabilities of positive selection and tabulated

amino acid replacements. These 14 highly variable sites were then mapped onto the crystal structure of Vif (Figure 2).

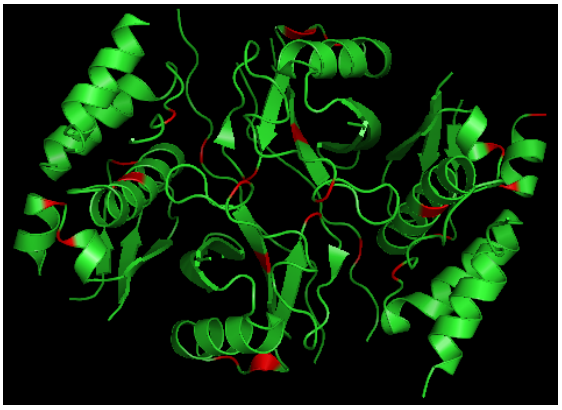

Figure 2: HIV1-Vif ribbon model. Red spots are residues undergoing positive selection.

Future literature search will reveal whether the sites under positive selection match with those suggested being involved in the Vif-APOBEC3G interaction. The information gained from this study may be useful in the design of therapeutic drugs by suggesting target residues that may weaken the Vif-APOBEC3G interaction and reduce Vif-induced degradation of APOBEC3G, leaving cells with their natural antiviral defense.

References

[1] J. Albin, (2010) "Interaction of host APOBEC3 restriction factors with HIV-1 in vivo: implications for therapeutics." Expert Reviews in Molecular Medicine, 12.4, 1-25.
[2] R. Holmes, (2007) "APOBEC3-mediated viral restriction: not simply editing?." TRENDS in Biochemical Sciences, 32.3, 118-128.
[3] J. Smith, (2009) "Multiple ways of targeting APOBEC3-virion infectivity factor interactions for anti-HIV-1 drug development." Cell, 638-646.
[4] Y. Suzuki, (2006) "Statistical properties of the methods for detecting positively selected amino acid sites." Gene, 365, 125-129.

The Effects of Entropy and Steric Hindrance on the Binding of O_2 to $Pd(IPr)_2$

Charles Lhermitte (Class of 2011)

Major: Chemistry
Principal Investigator: Dr. Carl D. Hoff
Department: Chemistry
Senior Thesis: Yes

The purpose of my research this past year was to study the difference in O_2 binding between two different Palladium complexes, $Pd(IMes)_2$ and $Pd(IPr)_2$. Most Pd compounds that bind O_2 bind it side-on (see Figure 1). $Pd(IMes)_2$ is a good example of such a compound. However, the $Pd(IPr)_2$ compound is able to bind two O_2 molecules in an end-on fashion (Figure 2). This is an important and new discovery. Learning more about why $Pd(IPr)_2$ is able to bind O_2 in this fashion is beneficial since, when O_2 is bound end-on it is in a superoxide state, while when it is bound side-on, it is a peroxide. In other words, when O_2 is bound end on as opposed to side on, it may be more reactive towards certain reagents. Thus $Pd(IPr)_2$ and other similar Pd compounds that can bind O_2 end on may have some potential as new catalysts.

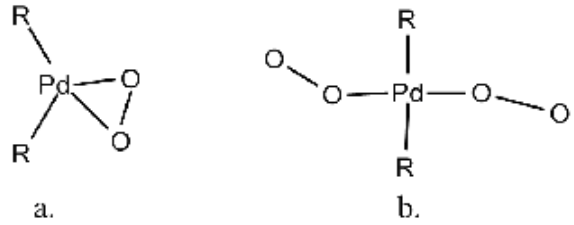

Figure 1: Binding of O_2 to Pd complexes. A) Represents side on binding. B) Represents end on binding.

In order to conduct this research Density Functional Theory (DFT) calculations were performed using Gaussian '03 software. DFT allows you to perform computations on the structures, energies and entropies of compounds by using principles in quantum mechanics. These methods were employed in order to answer why $Pd(IMes)_2$ was only able to bind O_2 side on at STP and why $Pd(IPr)_2$ was unable to

do so and preferred binding two O_2 molecules end on.

While conducting this research, it was suspected that this difference in binding between the $Pd(IPr)_2$ and $Pd(IMes)_2$was caused by a decrease in entropy (the measure of disorder in a system) and steric hindrance when O_2 was bound to the $Pd(IPr)_2$ compound. As you can see in Figure 2, the IMes group is a smaller ligand than the IPr. Because of this, the $Pd(IPr)_2$ compound has less room to move. When an O_2 molecule binds side on to a Pd complex such as $Pd(IMes)_2$ or $Pd(IPr)_2$, it 'squishes' the IPr or IMes ligands together due to repulsive forces between the electron clouds of the O_2 and the other ligands. Since the IPr ligand is much larger than the IMes, it does not have a lot of room to be 'squished' in that fashion. Figure 3[1] represents the Van Der Waals radii of the t-shaped adducts (only one O_2 atom is bound end-on) of $Pd(IPr)_2$ and $Pd(IMes)_2$, the green atom at the center is the Pd. In this figure is evident that there isn't much room for the O_2 to move in either molecule, however, for the $Pd(IPr)_2$ it seems almost impossible for the O_2 molecule to move into a side-on conformation.

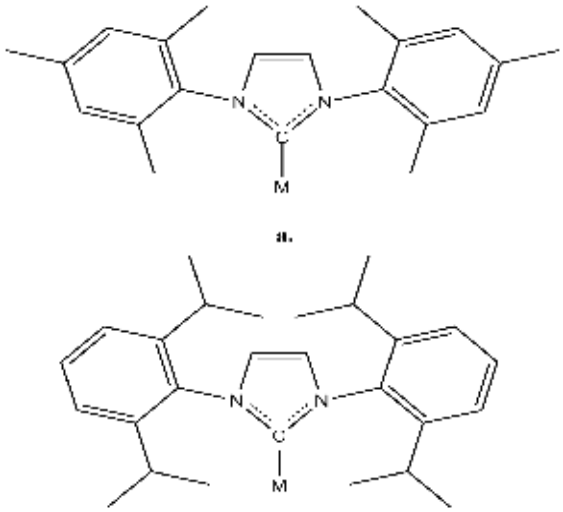

Figure 2: a. Represents the IMes ligand group and b. represents the IPr. As you can see, the location and size of the Isopropyl groups on the IPr ligand can place steric strain on the molecule and 'crowds' the area around the metal center (represented by M).

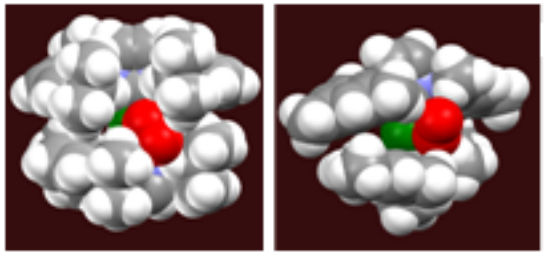

a. **b.**

Figure 3: This represents the Van Der Waals radii of the T-shapes species. **a.** is the T-shaped $Pd(IPr)_2$ compound and **b.** is the T-shaped $Pd(IMes)_2$. The green atom at the center represents Pd. As you can see, the $Pd(IPr)_2$ is significantly more crowded than the IMes variant, which prevents the molecule from rearranging to allow O_2 to bind side-on.

The results of the DFT calculations agreed that it was less favorable for the $Pd(IPr)_2(\eta^2\text{-}O_2)$ ($(\eta^2\text{-}O_2)$represents O_2 bound side-on) to form when compared to the formation of $Pd(IMes)_2(\eta^2\text{-}O_2)$; the calculated Gibbs free energy at 298K for the formation of the $Pd(IPr)_2(\eta^2\text{-}O_2)$ was +9.93 KCal/mol while the ΔG^0 For $Pd(IMes)_2(\eta^2\text{-}O_2)$ was -0.016 KCal/mol.This means that the side-on bound complex is disfavored at room temperature for the $Pd(IPr)_2$ but slightly favored for the $Pd(IMes)_2$. However, the calculated ΔS^0 (change in entropy) for the $Pd(IPr)_2(\eta^2\text{-}O_2)$ was -49.706KCal/mol*K while the ΔS^0 for the $Pd(IMes)_2(\eta^2\text{-}O_2)$ was -48.552 KCal/mol*K. Thus the loss in entropy for both in the formation of the $(\eta^2\text{-}O_2)$ is very similar. It turns out that the ΔH^0 (the enthalpy, or strength of the chemical bonds) for binding is what causes this difference in binding at room temperature. For the $Pd(IPr)_2(\eta^2\text{-}O_2)$ it is -7.15 KCal/mol while for $Pd(IMes)_2(\eta^2\text{-}O_2)$ it is -18 KCal/mol.

Although the DFT calculations revealed that it is in fact the ΔH^0 that is responsible for the $Pd(IPr)_2$'s inability to bind O_2 side-on at STP, it's structure is probably the cause of this. As it was pointed out earlier, the IPr ligands are much larger and, once bound to Pd, don't offer the molecule much "wiggle room." Thus it does not have many options in terms of structural conformations once an oxygen molecule binds side-on. Since the $\Delta H^0$of $Pd(IPr)_2$ is much higher than that of $Pd(IMes)_2$, this confirms that the $Pd(IPr)_2$ is forced into a high energy structure that is not stable at STP once O_2 binds side-on.

In conclusion, this DFT study revealed that the size of the ligands in Pd complexes can play a significant role in the binding of oxygen. This is important because by modifying ligands we may be able to develop, new reaction specific catalysts for the future. However, the first step before that would be to study more in depth the reactivity of such species in order to determine reactions that they could potentially catalyze.

References

[1] X. Cai, S. Majumdar, G. Fortman, C. Cazin, A. Slawin, C. Lhermitte, R. Prabhakar, M. Germain, T. Palluccio, S. Nolan, E. Rybak-Akimova, M. Temprado, B. Captain, C. Hoff (2011) "*Oxygen Binding to [Pd(L)(L')] (L= NHC, L' = NHC or PR3, NHC = N-Heterocyclic Carbene)*. Synthesis and Structure of a Paramagnetic Trans [Pd(NHC)2(η1-O2)2] Complex" J. Am. Chem. Soc., 133, 1290-1293

[2] B. Popp, V. Wendlandt, J.E. Landis, C.R. Stahl, and S.S Angew (2007) Chem. Int. Ed., 46, 601-604.

Function of Sts5 in Fission Yeast in the Regulation of Cell Growth

Jose Raul Perez (class of 2013)

Major: Microbiology and Immunology
Principal Investigator/Supervisor: Dr. Fulvia Verde
Department: Pharmacology
Senior Thesis: No

Surprisingly, little is known of how and why cells shape themselves the way they do. Recently, two genes have been discovered that could lead to answers concerning cell morphology, Orb6 and Sts5. By observing the phenotype of cells with an Orb6 mutant, Sts5 deletion, and a double mutant, which contains the Orb6 mutant and Sts5 deletion, the individual relationship the cells have with these genes, as well as how they work together, was noted. In this study we identified the genetic pathways in which these proteins work to control cell morphology.

Little is known about what genes influence the morphology of fission yeast cells or how they go about doing so. The morphology of cells indicates their function, which is why learning the mechanisms they use to shape themselves is so important. The reason this experiment was conducted on fission yeast is because several mammalian genes and their cellular functions are well conserved in fission yeast cells. Further, fission yeast cells have highly advanced genetic tools that allow us to study basic processes in biology. The genetic processes that fission yeast cells use to obtain a certain morphological shape is important because we could then link those genes with genes from mammalian cells to better understand how mammalian cells determine their shape.

The experiment was derived from previously known knowledge of the Sts5 gene (encoding a mRNA-binding protein) and the Orb6 gene (encoding a conserved kinase).[1] Dr. Fulvia Verde, my supervisor, had discovered some roles for these genes, both of which are involved in the shaping of yeast cells. By replacing these genes with mutant forms, thus hindering its function, or completely removingthe gene from the cell, we could see how the cell responded. Thus uncovering the function of that gene.[2]

We first analyzed the phenotype of a temperature sensitive mutant gene, *orb6-25*. These mutant cells at high temperature lose their shape and show defects in cell separation compared to normal cells, also known as "wild-type" cells.[2] The cells appeared smaller and more circular than a normal yeast cell, as depicted by Figure 1 to the left. Furthermore, at high temperatures the *orb6-25* mutants lose viability.[2] In comparison, when we deleted the *sts5* gene, denoted by *sts5*Δ, the cells became very large with aberrant cell shape as compared to the wild-type.

Interestingly, our studies detailed below show that the loss of viability phenotype of *orb6-25* [3] mutants is rescued by *sts5*Δ thus establishing a potential genetic interaction between Orb6 kinase and Sts5 protein. In Figure 2, cells of different dilution were grown on media that promotes cell growth.

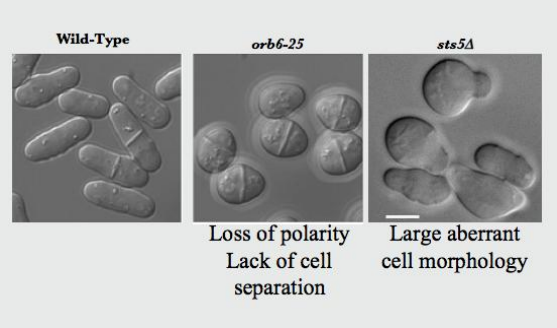

Figure 1: To the left is a photo of healthy Wild-Type cells. Middle photo shows small, circular yeast cells with *orb6-25*. To the right is a photo of disfigured cells with *sts5* deletion.

On each plate dilutions of the wild-type cells, *orb6-25* cells, *sts5*Δ cells, and the double mutant, *sts5*Δ *orb6-25*, were made. This allowed for proper examination of the phenotypes of each genetic strain. When grown at high temperature (36ºC) the phenotype of the wild-type, *orb6-25* and *sts5*Δ cells, were as expected. Wild-type cells grew well at 36 ºC while *orb6-25* cells did not grow at 36ºC. The *sts5*Δ cells also showed partial loss of growth at 36ºC. Interestingly the *orb6-25 sts5*Δ double mutant were able to grow better than the *orb6-25* and *sts5*Δ mutants alone. This suggests that *sts5* deletion rescues the *orb6* phenotype, and that these proteins work in the same pathway.

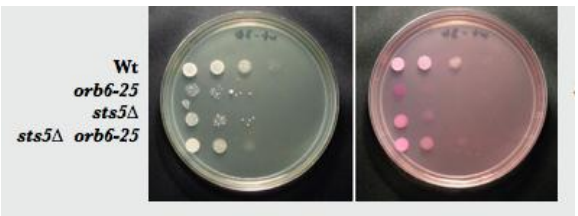

Figure 2: YE plates with strains in different dilutions and Phloxin B. The *orb6-25* and *sts5*Δ with most tint of pink.

Based on our observations, we hypothesized that Orb6 inhibits the function of Sts5, whose function is to promote mRNA degradation and thus to inhibit the translation of specific mRNAs as shown in Figure 3. In the absence of Orb6, Sts5 is no longer inhibited thus leading to mRNA being inhibited uncontrollably.

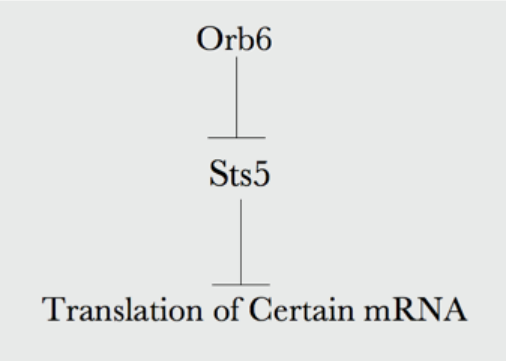

Figure 3: The hypothesized genetic pathway by which Orb6 and Sts5 operate.

With the *sts5*Δ, we hypothesized that the lack of inhibition of mRNA translation leads to increased levels of certain proteins occurring at inappropriate times, resulting in aberrant cell morphology and large cell size. Thus our results suggest that the role of Sts5 is to modulate the levels of specific mRNAs and of the corresponding proteins. Surprisingly we also observed that *orb6-25 sts5*Δ mutants did not show cell shape phenotypes similar to *orb6-25* or *sts5*Δ mutants but displayed a more normal cell shape. If indeed Sts5 is inhibited by Orb6 kinase then the *orb6-25 sts5*Δ double mutants should resemble the *sts5*Δ cells. Our results indicate that Orb6 kinase also controls cell morphology through an alternate pathway. This could explain why the *orb6-25 sts5*Δ cells did not become large and deformed. This discovery leads to the premise of future experimentation and a new understanding of fission yeast cell morphology control that has not been studied before.

Acknowledgement

I would like to thank Dr. Fulvia Verde for providing the lab and setting for this experiment to take place. I would like to also thank Dr. Maitreyi Das and Dr. David Wiley for being my mentors and instructors while performing this experiment. The Lemmon Laboratory for offering their microscope to take photos of the cells.

References

[1] F. Verde, D. J. Wiley, and P. Nurse. (1998). " Fission yeast orb6, a ser/thr protein kinase related to mammalian rho kinase and myotonic dystrophy kinase, is required for maintenance of cell polarity and coordinates cell morphogenesis with the cell cycle." Proc Natl Acad Sci U S A. 95(13):7526-31.

[2] M. Das, D. J. Wiley, X. Chen, K. Shah, and F. Verde (2009). "The Conserved NDR Kinase Orb6 Controls Polarized Cell Growth by Spatial Regulation of the Small GTPase Cdc42." Current Biology 19, 1314-1319.

[3] D. J. Wiley, S. Marcus, G. D'urso, and F. Verde (2003). "Control of Cell Polarity in Fission Yeast by Association of Orb6p Kinase with the Highly Conserved Protein Methyltransferase Skb1p." J. Biol. Chem. 278, 25256-25263.

The Relation Among Depressive Symptoms and Positive Imagery

Ashley Ramos (Class of 2010)

Major: Psychology
Principal Investigator/Supervisor: Dr. Jutta Joormann
Department: Psychology
Fellowship/Awards/Recognition: magna cum laude, General Honors, Departmental Honors
Senior Thesis: Yes

Major Depressive Disorder is the most commonly diagnosed mental illness in the United States today. The purpose of this study was to examine the relationship between depressive symptoms and the cognitive processing of positive stimuli. Participants were asked to listen to and imagine themselves in 100 emotionally positive scenarios, and were then assessed for depressive symptoms using the Center for Epidemiologic Studies Depression Scale (CES-D Scale; Radloff, 1977). Contrary to past research findings, data analyses revealed that depression scores were not significantly related to participants' abilities to vividly imagine positive situations. However, further research should be done with clinically depressed populations to further clarify this relationship.

Depression affects more people than any other psychiatric disorder, with a lifetime prevalence of 16.6%,[1] and is characterized by negative cognitive biases that facilitate negative world-views about an individual and the events he/she experiences.[2] Recent research has started to explore the relation between depression and the cognitive processing of positive stimuli. Holmes, Lang, and Shah (2009), for example,[3] demonstrated that participants who were trained to imagine positive scenarios were more resistant to a negative mood induction and scored lower on the tests used to predict the future onset of depressive symptoms. Along this line, researchers are now questioning whether this positive imagery training could be a practical form of therapy for individuals with Major Depressive Disorder (MDD). For my study, I attempted to replicate the experiment conducted by Holmes et al. to determine whether individuals with depressive symptoms, compared to those without, are less capable of imagining positive scenarios. Because the ability to imagine positive situations may serve as a protective barrier against depressive vulnerability, the relation between these two variables needed to be further examined and clarified.

Participants were asked to listen to and imagine themselves in 100 emotionally positive scenarios that begin ambiguously but consistently resolve in a positive manner. For instance, one scenario begins, "You are at home alone watching TV. You must have been dozing because you suddenly wake up. You have the impression that you heard a frightening noise and…" This sentence could end with a negative connotation (for example a burglar trying to enter the house), a neutral connotation (realizing that it was the television), or a positive connotation. Every scenario, however, finished in a positive manner, with this sentence specifically ending, "then realize with relief that it was your partner returning home".[4] Participants were instructed to keep their eyes closed while forming each of their mental images throughout the experiment. At the end of each scenario, participants were asked to rate how vividly they could imagine these scenarios on a scale from 1 *(not at all vivid)* to 5 *(extremely vivid).* We provided students with a printed copy of this scale to refer to throughout

the experiment. Students were then assessed for depressive symptoms using the Center for Epidemiologic Studies Depression Scale (CES-D Scale; Radloff, 1977). The CES-D is a 20-item questionnaire that asks participants to rate how frequently they had experienced various symptoms often associated depression in the past week. Based on previous research, I hypothesized that participants' levels of depressive symptoms would be negatively correlated with their vividness ratings for positive mental imagery. I also predicted that, at the beginning of the session, participants with more depressive symptoms would have lower vividness ratings, but that these scores would show greater improvements by the end of the experiment, compared with the vividness ratings of participants with fewer depressive symptoms.

Despite past evidence demonstrating the beneficial effects of positive imagery training on mood, the results of my correlation analysis suggest that depressive symptoms do not predict vividness ratings for positive imagery. In addition, a 2-way, repeated measures analysis of variance (ANOVA) showed that individuals with more depressive symptoms are equally successful at imagining positive scenarios as individuals with fewer symptoms, suggesting that they might not need or benefit from positive imagery training over time. In order to further clarify this relationship, future research should consider comparing clinically depressed populations with control populations to ensure that there are significant group differences.

One potential clinical application of research might be to examine the long-term effects of positive interpretation training on the maintenance of Major Depressive Disorder. For instance, researchers could hold several sessions in which depressed participants vividly visualize past, present, and prospective positive events, to examine whether positive imagery affects the course of depressive episodes.

Continued research on mood disorders, and specifically depression, is imperative. With nearly 17% of Americans affected, this high lifetime prevalence leads to many adverse effects for society, including the direct cost of treatment as well as indirect consequences, such as the loss of productivity on the workforce, stress on the families of depressed individuals, and some mortality. In 1990, the estimated social cost of depression in the United States was 43.7 billion dollars.[5] Though we have come a long way in terms of implementing evidence-based treatments, research on mental imagery represents a push for continual improvement and expansion in our approaches to treating mental illness.

References

[1] R. Kessler, P. Berglund, O. Demler, R. Jin,K. Merikangas, And E. Walters (2005). "Lifetime prevalence and age-of-onset distributions of DSM-IV disorders in the national comorbidity survey replication" Archives of General Psychiatry, 62, 593-602.
[2] A. M. Kring,G. C. Davison, J. M. Neale, and S. L. Johnson (2007). "Mood disorders. In C. T. Johnson (Ed.)" Abnormal Psychology (10th Ed.). (229-269). John Wiley & Sons.
[3] E. A. Holmes, T. J. Lang, and D. M. Shah, D. M. (2009). "Developing interpretation bias modification as a cognitive vaccine for depressed mood: Imagining positive events makes you feel better than thinking about them verbally" Journal of Abnormal Psychology, 118, 76-88.
[4] E. A. Holmes, A. Mathews, T.Dalgleish, and B. Mackintosh (2006). "Positive interpretation training: Effects of mental imagery versus verbal training on positive mood" Behavior Therapy, 37, 237-247.
[5] P. Greenberg, L. Stiglin, S. Finkelstein, and E. Berndt (1993). "The economic burden of depression in 1990" Journal of Clinical Psychiatry, 54, 405-418.

Using Distant Galaxies in Cosmic Microwave Background Data to Analyze the WMAP Beam Model

Kasey Schultz (Class of 2012)

Majors: Physics and Mathematics
Principle Investigator/Supervisor: Dr. Kevin Huffenberger
Department: Department of Physics, University of Miami
Fellowship/Awards/Recognition: Beyond the Book Research Scholarship, Honors Summer Research Program
Senior Thesis: No

The sensitivity and resolution of the Wilkinson Microwave Anisotropy Probe (WMAP) have recently been called into question. The focus of the scrutiny is on the model of the beam generated by observing Jupiter. These differences in the instrument, if true, would imply noticeable shifts in the values of cosmological parameters obtained through WMAP data, including measurement of the relative amounts of dark matter, dark energy and normal matter in the universe as well as the universe's overall geometry. The purpose of this study is to statistically analyze the effective beam as recovered through observing point sources of radiation--distant galaxies--in the CMB maps produced by WMAP and to also find the cause of any deviations of the effective beam from the Jupiter model.

The Cosmic Microwave Background (CMB) is the relic light of the Big Bang that gives us a glimpse of the first moments of our universe. This background radiation comes from around 400,000 years after the Big Bang when the universe had cooled sufficiently for the first atoms to form from the initial hot, opaque plasma of elementary particles. At this time light was first able to move freely throughout the universe. These first propagating photons are the CMB and the first observable light. By studying tiny variations in the temperature of the CMB across, one can find the clues to the universe's large scale structure and to the relative amounts of dark matter, dark energy, and normal matter found in the universe.

The Wilkinson Microwave Anisotropy Probe (WMAP) is a CMB-observing satellite currently in orbit around the sun, constantly in Earth's shadow. Equipped with high precision instruments, WMAP measures the CMB in a total of 5 frequency bands from about 20 to 90 GHz. In order to calibrate these instruments after WMAP's launch, a series of observations of the planet Jupiter were done in order to create a mathematical model of the sensitivity and resolution of the instruments. The accuracy of this model strongly impacts the accuracy of the data obtained, and cosmological interpretation thereafter.

Figure 1 shows the CMB as observed by WMAP, and Figure 2 shows a distant galaxy (point source) that emits radiation of similar

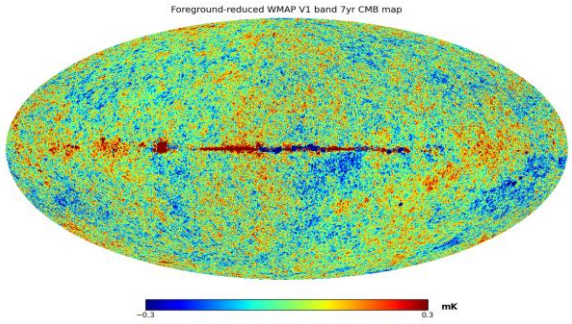

Figure 1: The CMB as seen by WMAP with a model of the galactic foreground contamination from the Milky Way removed. The remaining red band is residual galactic contamination.

wavelength to the CMB that contaminates the map. These galaxies are incredibly distant and thus point-like, but on CMB maps they appear smoothed out over multiple pixels. The degree to which these points are smoothed depends on the size of WMAP's beam; the wider the beam, the more smoothed out the point sources will be. In measuring the amount of smoothing, averaged over all point sources, one gets an accurate representation of WMAP's actual beam.

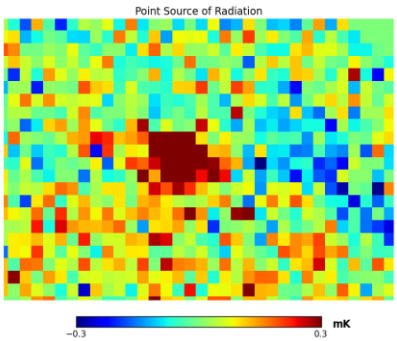

Figure 2: A single point source

Sawangwit and Shanks (2010) claim that by using this method to estimate the beam, they are unable to get a good fit to the Jupiter-modeled beam. They show that the estimated beam shows many noticeable offsets above its modeled counterpart. I was able to reproduce this result, shown in Figure 3.

To estimate WMAP's beam I first computed a radial temperature profile for each

distant galaxy in the WMAP catalog (list of identified point sources by WMAP). I then averaged the individual profiles together. The pixels in the CMB map around each point source are combined with respect to their distance from the source center. The resulting radial temperature profile is visualized by plotting temperature as a function of the angle from the source. The usable information comes when I average the profiles of all the sources together (the stacked profile) and compare this with the modeled beam from Jupiter observations. The result of fitting the beam to the stacked profile by modulating the amplitude is shown in Figure 3; the residuals (data – model) are shown in Figure 4.

Figures 3 and 4 show that an amplitude-only fit is not sufficient. In order to get a better fit to the data we used a 4-parameter model for the beam; one modulated the amplitude (A), one was a vertical offset (m_0) and the other two controlled the width (σ, ε). The model can be represented as:

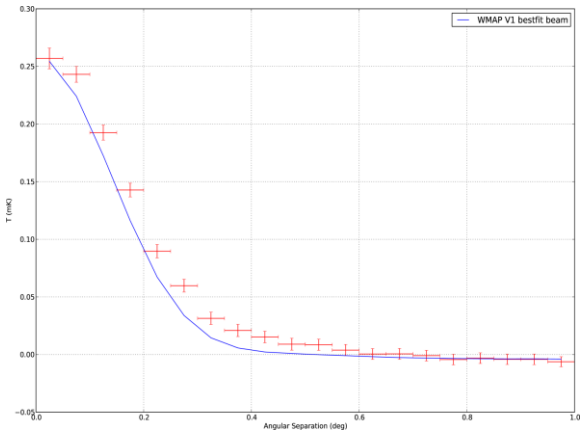

Figure 3: From WMAP CMB map shown in Figure 1, the stacked profile (red error bars) plotted against an amplitude-only fit (black line), note the discrepancy. This plot is only for V1 frequency, but preserves generality (true for all single-curve plots in this article).

$$m(\Theta) = A(b*g_{\sigma a})(\Theta) + m_0$$

and

$$\sigma_a = \sigma(S_V/1Jy)^{\varepsilon}$$

where Θ measures angular separation on the sky, $m(\Theta)$ is the model constructed from the various parameters, $b*g_{\sigma a}$ denotes the convolution of the estimated beam with an adjustable width Gaussian curve, and σ_a is the adjustable width of the Gaussian as the map standard deviation (σ) multiplied by a source flux power law.

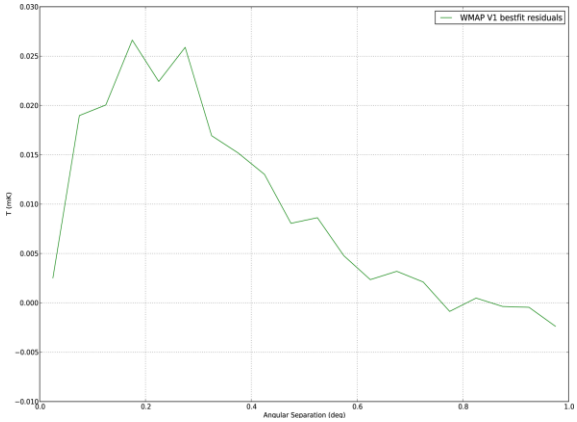

Figure 4: The difference between the best-fit modeled beam and the effective beam computed from the radial

Although this four parameter model provides a good fit, the optimized parameters (corresponding to different physical phenomena leading to a wider estimated beam) are physically inconsistent and as such these parameters provide an invalid explanation. The inconsistency in the optimized parameters tell us that we can rule out the following physical phenomena to explain the broad stacked profiles: a band-pass effective frequency for the detectors, a positional uncertainty in the locations listed in the WMAP point source catalog, and a flux dependency of the effective beam width.

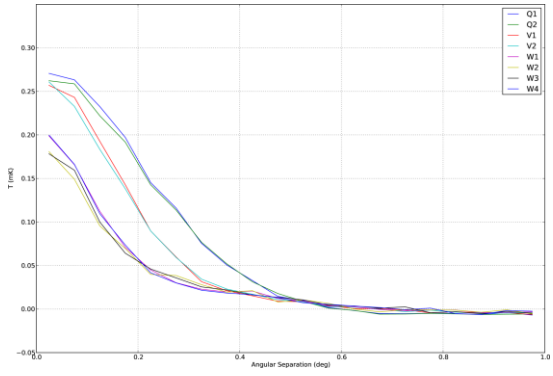

Figure 5: The stacked profiles for each WMAP frequency.

In looking at Figure 5 we noticed that all profiles seem to lie on a common "lump." We attribute this to the fact that a dimmer source with brightness just below the detection limit

can get a "boost" above this threshold by lying directly in line with a positive CMB fluctuation. Therefore a dim source is more likely to be in the catalog if this boosting has happened, which might produce a common structure due to the CMB fluctuation. This is supported by the fact that we observe, when looking at the profile for an individual source, dimmer sources have broader profiles.

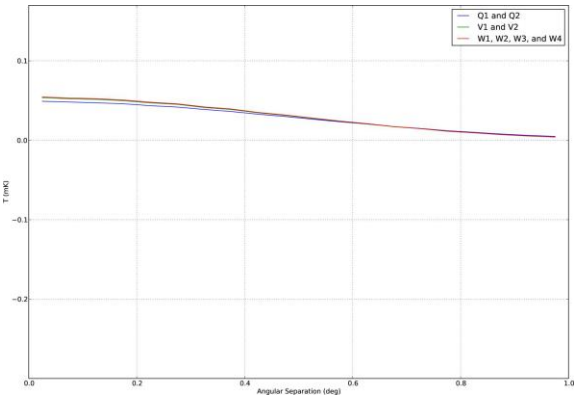

Figure 6: Simulated effect of common CMB fluctuation that boosts dim sources into WMAP catalog and broadens effective profile.

In order to estimate what effect this CMB boosting would have on the data, I ran CMB simulations. For random points on the sky, I generated a temperature profile for those points with a positive CMB fluctuation. I then averaged this over 100 simulated maps, using 1000 random points per map; the result is shown in Figure 6.

If this CMB fluctuation is responsible for the broad stacked profiles, then these simulations should approximate the residuals of the best-fit plot (Figure 7). Said differently, the simulations should look like the excess in the profiles. Figures 6 and 7 seem to indicate that this common CMB fluctuation matches the stacked profile discrepancy outlined in the Sawangwit and Shanks' paper. This is visualized by comparing the shapes and amplitudes of Figures 6 and 7 to the common feature in Figure 5.

In order to further strengthen our argument for a statistical bias (the common CMB fluctuation), I ran the same profiling technique to estimate the effective beam from a different point source catalog produced by the NVSS mission. If the broadness of the estimated beam is due to a statistical bias in the WMAP catalog, then the broadness will be absent from profiles generated from NVSS selected.

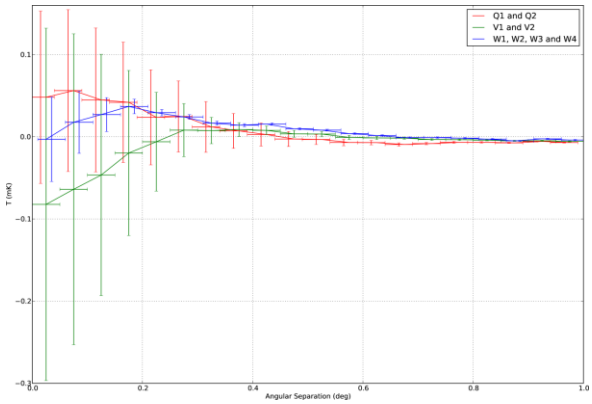

Figure 7: The residuals from amplitude-only fitting for each WMAP frequency band, compare to CMB fluctuation simulations in Figure 6.

This is due to the fact that NVSS can see much dimmer sources, has a much lower selection threshold, and has a much finer resolution than WMAP. The results of the NVSS selected source analysis are shown in Figures 8 and 9. Figure 4 shows that there is a significant structure to the residuals from WMAP selected sources (due to CMB fluctuation) while Figure 9 shows that the residuals from the NVSS selected sources show no such structure.

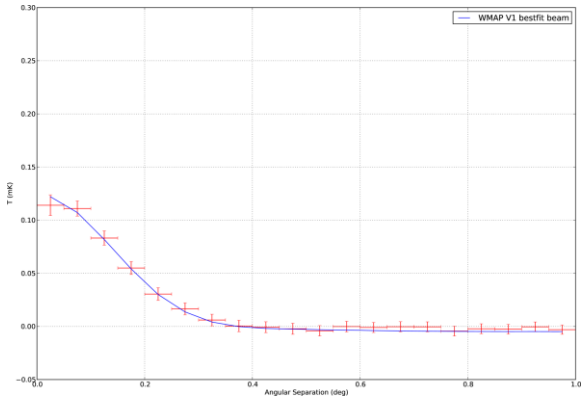

Figure 8: Amplitude-only fit for NVSS selected sources on the same WMAP CMB maps. Note the much better fit than Figure 3.

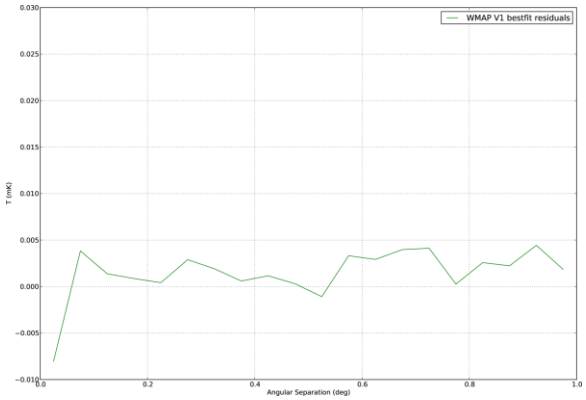

Figure 9: Residuals for amplitude-only fitting of WMAP modeled beam to NVSS selected source profile, almost trivial.

A third consistency check arose when the WMAP team released a "CMB-free" point source catalog. This was a more carefully selected catalog in which, before identifying sources in each frequency band, the team combined the three highest resolution frequencies in such a way to remove the CMB. Then identifying sources in this combined map ensures no CMB-related bias in the catalog. I again ran the profiling routines on these sources and got a better fit to the modeled beams, however it was still not quite as good as the NVSS selected sources. This can be loosely translated as: compared to the original WMAP catalog, the fit to the modeled beam from the WMAP CMB-free sources is twice as good, and the fit to the beam from the NVSS sources is four times as good.

We have evidence that there is a statistical bias in the WMAP catalog selection that is not present in the WMAP CMB-free catalog, nor is it present in the NVSS catalog. Furthermore my simulations show that CMB fluctuations along the line of sight to dim sources can boost their flux above the catalog detection threshold and result in a common fluctuation in the stacked profiles. This common fluctuation can then lead to a poor fit between the stacked profiles and the beam models. I am currently working on simulating point source detection and catalog reconstruction to further verify these preliminary results.

References

[1] Hill R. S., et al., 2009, "Five-Year Wilkinson Microwave Anisotropy Probe (WMAP) Observations: Beam Maps and Window Functions", ApJS, 180, 246-264

[2] Sawangwit U., Shanks T., 2010, "Beam profile sensitivity of the WMAP CMB power spectrum", MNRAS letter

[3] E. Wright, et al., 2009, "Five-Year Wilkinson Microwave Anisotropy Probe (WMAP) Observations: Source Catalog," ApJS, 180, 283-295

Lady Liberty: Influence of Goals and Energy on Distance Perception

Sana Sherali (Class of 2012)

Major: Psychology and Human and Social Development (Track I)
Principal Investigator/Supervisor: Dr. Emily Balcetis
Department: Social Psychology of New York University
Fellowship/Awards/Recognition: Social Perception and Action Motivation Lab Internship (Summer 2010)
Senior Thesis: No

In this study, the interplay of goals and energy upon distance perception to participants visiting the Statue of Liberty was examined. We measured goal commitment, energy, and distance perception to the Statue of Liberty. When participants had low goal commitment, they perceived the Statue of Liberty to be far away. However, participants perceived the Statue of Liberty to be closer when their goal commitment to reach Lady Liberty was high, regardless of their energy level. This study suggests that goals and energy interact to influence how we perceive distance, implying that a psychological goal may be able to make up for a lack of physical energy.

In this article, we explore two factors that influence perception: energy and goals. It has been shown that energy influences how people view their environment. For example, people tend to view hills as steeper once they have jogged vigorously for an hour[1] which

suggests that when an individual's energy level is low, environments are perceived as more extreme. Furthermore, Balcetis and Dunning[2] have found that desirable objects appear closer than less desirable objects. Their study suggested that perceptual processes are biased towards a person's goals. In other words, individuals view the world in favor of their own desires. With these results in mind, we decided to test if psychological goals can make up for a lack of physical energy, in which case, having a goal could possibly make up for low energy thereby allowing an individual to accomplish his or her goals regardless of energy level.

In order to explore these factors, we recruited 61 individuals from two areas that were equidistant from the Statue of Liberty at Battery Park, New York. The surveys measured the participants' energy by having each participant self-report his or her chronic energy level. A description of the participants' fatigue level was also collected. Energy was calculated as an aggregate energy score that defined a participant's level of chronic energy. The aggregate chronic energy score was calculated by averaging the results from two questions that asked about fitness (usual feeling of fitness and physical condition) with the results from three questions that asked about fatigue (easily fatigued, fatigue interference, and frequency of fatigue problems). Once this average was calculated, the fatigue factor was subtracted from the fitness factor. This gave us a composite score of how fit the participants were in general minus how fatigued they felt.

To assess whether participants did or did not have the goal to get to the Statue of Liberty, we asked if the participant was "going to take the ferry to the Statue of Liberty later today." In order to assess perception of distance, we asked participants to indicate how many feet separated them from the Statue of Liberty. The surveys differed in the order of the location questions.

To explore the relationship between goals, energy, and distance perception, we ran a regression predicting distance estimates from energy, goals, and the interaction between the two. The overall model had a low significance of $R^2 = .147$, $F(3, 48) = 2.759$, $p = .052$. The main effect of goal was not significant, $\beta = -.119$, $t(56) = -.878$, $p = .384$. The main effect of energy was not significant, $\beta = -.186$, $t(56) = -1.369$, $p = .177$. However the interaction between goal and energy was significant, $\beta = -.325$, $t(56) = 2.434$, $p = .019$.

As shown in Figure 1, among people without the goal to reach the Statue of Liberty, distance perception to the Statue of liberty decreased as energy increased. Among people with the goal to reach the Statue of Liberty, energy had no effect on the perception of distance. Instead, people with the goal perceived the Statue as close regardless of their level of energy. When looking at the interaction, it becomes apparent that having a goal truly matters for individuals who have low energy. Individuals with a goal and low energy are viewing the Statue of Liberty as closer than individuals with no goal and low energy. This indicates that, somehow, having a goal is making up for the lack of physical energy an individual has.

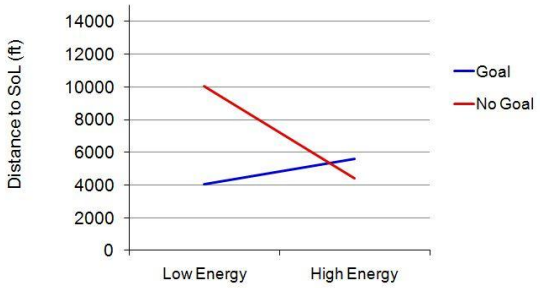

Figure 1: Interaction between energy level and goal.

Our findings suggest that a psychological goal may be able to make up for the lack of physical energy. That is, among the participants who had low energy but a goal to visit the Statue of Liberty, distance was perceived as shorter. Future research will explore whether our goals form a type of "psychological energy" that compensates for the lack of our physical energy. When considering the concept of a psychological goal and the role it plays in compensating for energy, many potential applications of this theory appear. This notion could be applied to academics, dieting, depression, and many other life situations. Looking specifically at dieting, we plan to question why individuals have such great difficulty losing weight. Could their goals be manipulated in a manner to assist in making the

distance they need to walk or run for exercise appear closer than it may actually be? "Psychological energy" can compensate for a lack of physical energy causing goals to be perceived as closer than they may actually be.

References

[1] M. Bhalla, and D.R. Proffitt (1999). "Visual Motor Recalibration in Geographical Slant Perception" Journal of Experimental Psychology, Human Perception and Performance 2 25, 1076-096.

[2] E. Balcetis & D. Dunning (2010)."Wishful seeing: Motivational influences on visual perception of the physical environment" in E. Balcetis, & G. D. Lassiter (Eds.), The social psychology of visual perception. New York: Psychology Press.

Stress Recovery in Depression: Why Emotion Regulation Matters

Mary L. Woody (Class of 2011)

Major: Psychology& Women and Gender Studies
Principal Investigator/Supervisor: Dr. Jutta Joormann and Joelle LeMoult
Department: Psychology
Fellowship/Awards/Recognition: Beyond the Book Scholarship
Senior Thesis: Yes

This study investigated the effects of rumination on psychological and biological recovery from stress in currently depressed participants (MDD) and never-depressed control participants (CTL). Following a baseline period, participants were exposed to (1) a three-part psychosocial stressor, (2) a randomly assigned emotion-regulation (ER) task (distraction or rumination), and (3) a recovery period. Psychological and biological reactivity and recovery were measured by self-reported anxiety ratings and respiratory sinus arrhythmia (RSA). There were no group differences in self-reported anxiety, but there was, however, a significant interaction between time, condition, and group in RSA. MDDs but not CTLs' RSA fluctuations were affected by their ER condition.

Researchers are delineating the variables that make an individual vulnerable to depression. Individuals diagnosed with major depressive disorder (MDD) often display biocognitive vulnerabilities to negative affect[1] and have difficulty regulating emotional and biological states during and after stressful situations.[2]

To examine the biological effects of psychosocial stressors, psychologists measure respiratory sinus arrhythmia (RSA), the natural variation in heart rate primarily driven by breathing patterns and the regulating influence of the vagus nerve on the heart. In general, RSA levels are highest at rest and decrease in response to stress. Subsequent increases in RSA are crucial for restoring biological homeostasis after a stressful event, and depressed individuals show less RSA response after a stressful situation than do healthy individuals.[3]

Recent studies have sought to identify factors that inhibit recovery from stress and, thus, make some individuals more vulnerable to depression. Thompson[4] proposed that the emotional regulation style used during stress is one such vulnerability factor. Two of the most commonly studied emotion regulation styles in MDD are rumination (perseverative thoughts about a problem) and distraction.

RSA: REPEATED MEASURES ANOVA

Interaction	df	Mean square	F-value	Significance
Time by Group by Condition	2	0.374	4.032	0.024
Follow-up: MDD only Time by Condition	1	0.266	6.753	0.020
Follow-up: CTL only Time by Condition	1	0.013	0.112	0.741

RSA: MDD DISTRACTION CONDITION PAIRED SAMPLES T-TEST

Results	AS - ER1	ER1 - ER2	ER2 - R1	R1 - R2	ER1 - R2	ER2 - R2
Mean	0.376	0.045	-0.292	-0.345	-0.579	-0.624
t-Statistic	2.920	0.311	-1.234	-2.085	-3.338	-3.356
df	8	8	7	7	8	8
Sig. (2-tailed)	0.019	0.764	0.257	0.076	0.010	0.010

RSA: MDD RUMINATION CONDITION PAIRED SAMPLES T-TEST

Results	AS - ER1	ER1 - ER2	ER2 - R1	R1 - R2	ER1 - R2	ER2 - R2
Mean	0.421	0.013	-0.485	0.144	-0.327	-0.341
t Statistic	2.505	0.237	-4.808	1.172	-2.009	-1.942
df	8	8	8	8	8	8
Sig. (2-tailed)	0.037	0.818	0.001	0.275	0.079	0.088

Table 1: Results of repeated measures ANOVA and paired samples t-test by group.

Research has shown that individuals who ruminate while stressed prolong recovery and become more vulnerable to depressive disorders.[5]

Although many studies have exposed depressed participants to acute laboratory

stressors, most examine only the cognitive consequences of emotion regulation. The aim of the current study is to analyze the effects rumination on biological and psychological recovery in MDD and control (CTL) participants. To examine the biological stress response and recovery, following a baseline period, participants were exposed to (1) a three-part psychosocial stressor, (2) a randomly assigned emotion-regulation (ER) task (distraction or rumination), and (3) a recovery period. Psychological and biological reactivity and recovery were measured by self-reported anxiety ratings and respiratory sinus arrhythmia (RSA).

To examine reactivity and recovery from stress, a mixed-effects measures analysis of variance (ANOVA) was conducted with group (MDD, CTL) and condition (rumination, distraction) as the between-subject factors and time as the within-subject factor. The results indicated that there were no group differences in self-reported anxiety. There was, however, a significant interaction between time, condition, and group in RSA values. MDDs' but not CTLs' RSA changes were affected by their ER condition (see Table 1). MDDs in both conditions showed equivalent biological reactivity to the ER condition and equivalent initial recovery during the recovery period. However, whereas MDD participants in the distraction condition showed continued biological recovery over time, those in the rumination condition failed to show continued improvement (see Figure 1).

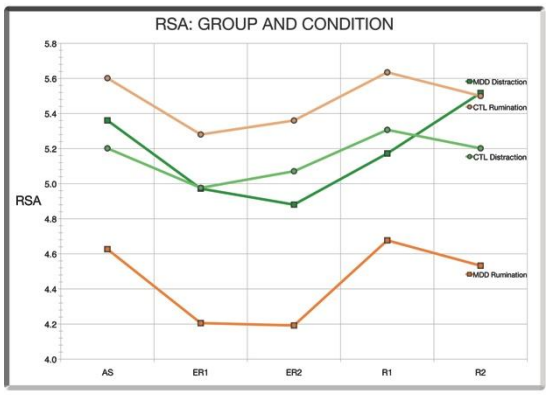

Figure 1: Graph of RSA recovery by group and condition.

As hypothesized, these results suggest that the use of rumination may hinder continued biological recovery from stress in depression. These results indicate that rumination is a mechanism underlying the prolonged biological response to stress in depression and, therefore, may increase vulnerability to depression. Future studies should further examine the effects of rumination on biological recovery and look at emotion regulation strategies other than rumination. Additionally, future research should analyze these processes in other disorders, such as anxiety disorders.

References

[1] R. Kessler, P. Berglund, O. Demler, R. Jin, K. Merikangas, and E. Walters, (2005). "Lifetime Prevalence and Age-Of-Onset Distributions of DSM-IV Disorders in the National Comorbidity Survey Replication" Archives of General Psychiatry, 62, 593-602.
[2] M. Flynn, and K. Rudolph (2007). "Perceptual Asymmetry and Youths' Responses to Stress: Understanding Vulnerability to Depression" Cognition and Emotion, 21, 773-788.
[3] J. Rottenberg, A. Clift, S. Bolden, and K. Salomon (2007). "RSA Fluctuation in Major Depressive Disorder." Psychophysiology, 44, 450-458.
[4] R. Thompson, (1994). "Emotion Regulation: A Theme in Search of Definition" Monographs of the Society for Research in Child Development, 59, 250-283.
[5] N. Just, and L. Alloy (1997). "The Response Styles Theory of Depression: Tests and an Extension of the Theory" Journal of Abnormal Psychology, 106, 221-229.